



ELSEVIER

Nuclear Instruments and Methods in Physics Research B 161–163 (2000) 354–358

**NIM B**  
Beam Interactions  
with Materials & Atoms

www.elsevier.nl/locate/nimb

# Mapping of light elements with the ANSTO high energy heavy ion microprobe

Rainer Siegle<sup>\*</sup>, David D. Cohen

*Australian Nuclear Science and Technology Organisation, PMB 1, Menai 2234, NSW, Australia*

---

## Abstract

7.62 MeV He was used to study the distribution of a wide range of elements in mineral sands. At this energy both He induced X-ray emission and a high energy resonance in oxygen can be applied simultaneously. The two techniques were used to study the distribution of elements ranging from sulfur to zirconium as well as oxygen. © 2000 Elsevier Science B.V. All rights reserved.

*PACS:* 82.80.Yc

*Keywords:* Ion microprobe; IBA

---

## 1. Introduction

Recently a new high energy, heavy ion microprobe [1] has been installed at the Australian Nuclear Science and Technology Organisation (ANSTO). The aim was not to duplicate existing proton microprobe facilities in Australia or internationally, but to design a microprobe that can utilise high energy IBA techniques using heavy as well as light ions. The high energy heavy ion microprobe at ANSTO was designed to focus ions with a mass energy product of  $ME/q^2 = 100$  MeV amu. This enables us to use IBA techniques that have previously not been extensively used on ion

microprobes. These include the high energy  $^{16}\text{O}(\alpha, \alpha)^{16}\text{O}$  resonance at 7.30–7.65 MeV. Nuclear resonances and reactions are mainly used to analyse a range of light elements such as H, C, N and O. Our aim is to establish the use of ion beam techniques other than PIXE and RBS on an ion microprobe. The main emphasis is to use moderate beam spot sizes between 5 and 20  $\mu\text{m}$  with sufficient beam current to perform an analysis in a reasonable time.

Extremely strong  $(\alpha, \alpha)$  resonances of even–even nuclei are particularly useful for the measurement of  $^{12}\text{C}$  and  $^{16}\text{O}$ . The use of these resonances for the analysis of carbon and oxygen has previously been demonstrated by Davies et al. [2,3]. However, using this resonance alone is not very useful since only oxygen and the heavy elements, for which the scattering cross sections are still Rutherford, can be measured with this technique. Therefore we

---

<sup>\*</sup> Corresponding author. Tel.: +61-2-9717-3967; fax: +61-2-9717-3257.

*E-mail address:* rns@ansto.gov.au (R. Siegle).

have combined this technique with helium induced X-ray emission (HIXE) to be able to map a broad range of elements in one measurement. In this paper we demonstrate that both techniques, which cover a complementary range of elements, can be used simultaneously.

## 2. Experimental

The high energy heavy ion microprobe [1] is installed on a 10 MV tandem accelerator. The belt charging system of the accelerator was recently upgraded to a pelletron system, which improved the terminal voltage stability to less than 1 kV at 8 MV, which is required for a microprobe. The tandem accelerator is equipped with two sputter ion sources and a charge exchange RF ion source. Most elements of the periodic table can be accelerated with reasonably high intensity by these ion sources.

The major components of the microprobe were supplied by Oxford Microbeam. The microprobe lens system consists of a magnetic quadrupole triplet, which provides enough focussing power to focus ion beams with a  $ME/q^2$  of up to 100 MeV amu at a working distance of 150 mm. The beam scanning system can raster the ion beam over an area of up to  $1 \times 1 \text{ mm}^2$ . The target chamber is equipped with a microscope for sample alignment and various detectors. These include a surface barrier detector for RBS, a Peltier cooled Si PIN diode as X-ray detector and a large solid angle dE-E telescope, which is used for heavy ion elastic recoil detection analysis.

The X-ray detector is located about 75 mm from the target at a  $135^\circ$  angle relative to the forward direction of the incoming beam. In order to prevent scattered ions from entering the detector it was fitted with a 50  $\mu\text{m}$  thick Kapton foil. A surface barrier detector for the detection of the scattered particles is installed at a  $165^\circ$  angle relative to the beam. This detector is located 75 mm from the target and covers a solid angle of 8 msr. This relatively large solid angle for an RBS detector is required because of the small beam currents available at small spot sizes.

The samples were analysed with both He induced X-ray emission and RBS using a 7.62 MeV He beam. At this energy  $^{16}\text{O}$  shows a broad resonance with a cross section that is  $\sim 100$  times greater than that for Rutherford scattering [2,3]. At the same time this energy is well suited for X-ray fluorescence analysis, since He has a high X-ray excitation cross section. All samples were measured with the beam at normal incidence. In all the measurements the ion beam was focussed to spot sizes between 10 and 15  $\mu\text{m}$ , which was confirmed by scanning over the edge of a Au-layer deposited on a silicon wafer.

In order to demonstrate the simultaneous use of He induced X-ray emission and  $(\alpha, \alpha)$  resonance analysis, specimens of mineral sands were prepared. The samples consisted of a mixture of grains of ilmenite ( $\text{TiFeO}_3$ ), pyrite ( $\text{FeS}_2$ ), rutile ( $\text{TiO}_2$ ), magnetite ( $\text{Fe}_3\text{O}_4$ ) and zircon ( $\text{ZrSiO}_4$ ). This covers a wide range of elements, which will enable us to evaluate whether a combination of the two techniques can cover a wider range of elements. The size of the grains in the specimen is between 50 and 300  $\mu\text{m}$ . In order to be able to analyse the sample with the microprobe the grains were fixed on a graphite sheet with organic spray glue.

## 3. Results and discussion

Fig. 1 shows a typical X-ray spectrum of the specimen. The spectrum was taken with 7.62 MeV He ions and is the total spectrum for a scan over a  $1 \times 1 \text{ mm}^2$  area. The spectrum clearly shows X-ray peaks for titanium, chromium, iron, zirconium and sulfur. Sulfur is only just visible in the spectrum because of the small fraction of pyrite in the mineral sand mixture. Further, the S peak overlaps with the Ti escape peak.

The maps of the major elements corresponding to the above spectrum are shown in Fig. 2. The maps show the number of X-rays at the characteristic energy for these elements covering an area of  $1 \times 1 \text{ mm}^2$ . The maps clearly show the individual grains in the sample. From these maps some of the minerals present in the sample can readily be distinguished. For example, from the sulfur and

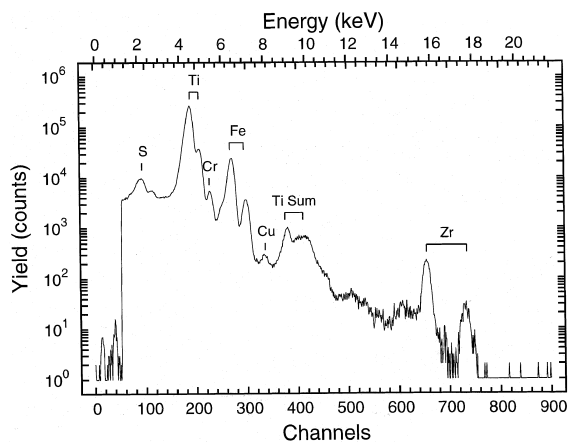


Fig. 1. Total X-ray spectrum of a scan over a  $1 \times 1 \text{ mm}^2$  area on a mineral sands specimen, containing grains of ilmenite ( $\text{TiFeO}_3$ ), pyrite ( $\text{FeS}_2$ ), magnetite ( $\text{Fe}_3\text{O}_2$ ), zircon ( $\text{ZrSiO}_4$ ) and rutile ( $\text{TiO}_2$ ). Clearly visible are the X-ray peaks of the major elements S, Ti, Fe and Zr in the mineral.

iron maps, the pyrite grains can easily be identified. As expected, at locations with high Fe and S concentrations none of the other elements are present. However, the sulfur maps also show a high count rate in areas where Ti and Zr is present. At locations where Zr is present, this is due to the Zr L-lines, which appear at an energy close to the sulfur K-lines. Fig. 3 shows a spectrum taken as a spot measurement on the zircon grain in the upper right corner. The spectrum clearly shows the major elements of zircon, Zr and Si, but also traces of hafnium, which is known to be present in zircon. The Fe and Ti visible in the spectrum are due to the scattered beam hitting one of the neighbouring grains.

Fig. 4 shows the backscattering spectrum taken simultaneously with the X-ray spectrum of Fig. 1. The part of the backscattering spectrum originat-

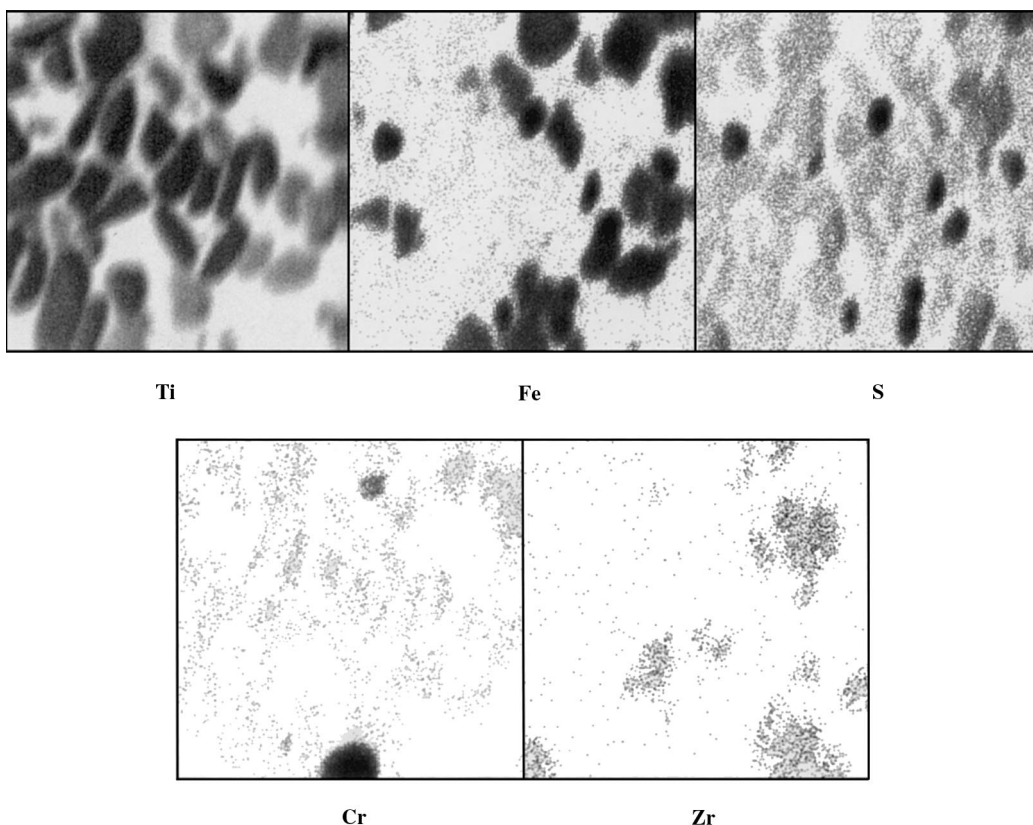


Fig. 2. Elemental maps of titanium, iron, sulfur, chromium and zirconium in a mineral sands specimen taken from X-ray spectrum. The area of the scan is  $1 \times 1 \text{ mm}^2$ .

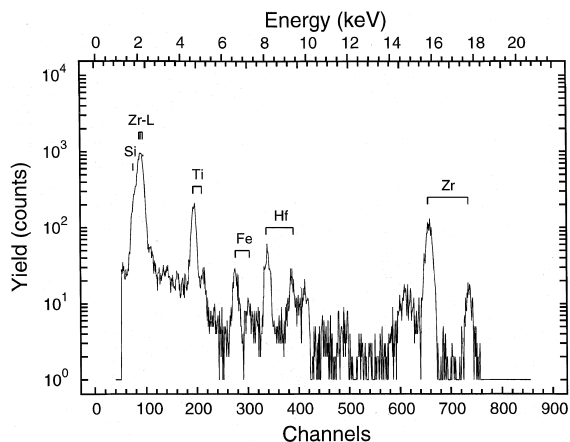


Fig. 3. X-ray spectrum of a spot measurement on the zircon grain visible in the upper right corner of Fig. 2.

ing from light elements is no longer Rutherford, due to the high energy of the incident beam, which results in the large peaks in the low energy part of the spectrum. Indicated in the figure are the energies for the particles backscattered from different elements at the surface. The surface edges for Zr, Fe, Ti and Si are clearly visible. However, the Fe

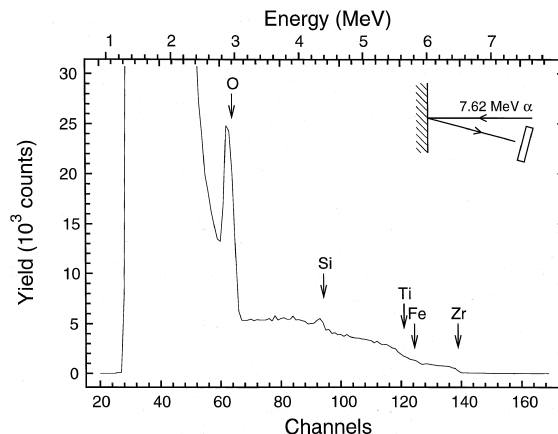


Fig. 4. Backscattering spectrum of mineral sands specimen taken with 7.62 MeV He. The edges for Zr and the O peak, which has the enhanced cross section at this energy, are clearly visible.

and Ti edges are less pronounced, because of the proximity of the two elements together with the large solid angle of the detector. The scattering of both Si and O are no longer Rutherford, which causes the structure in the spectrum at lower energies. However, the much enhanced cross section

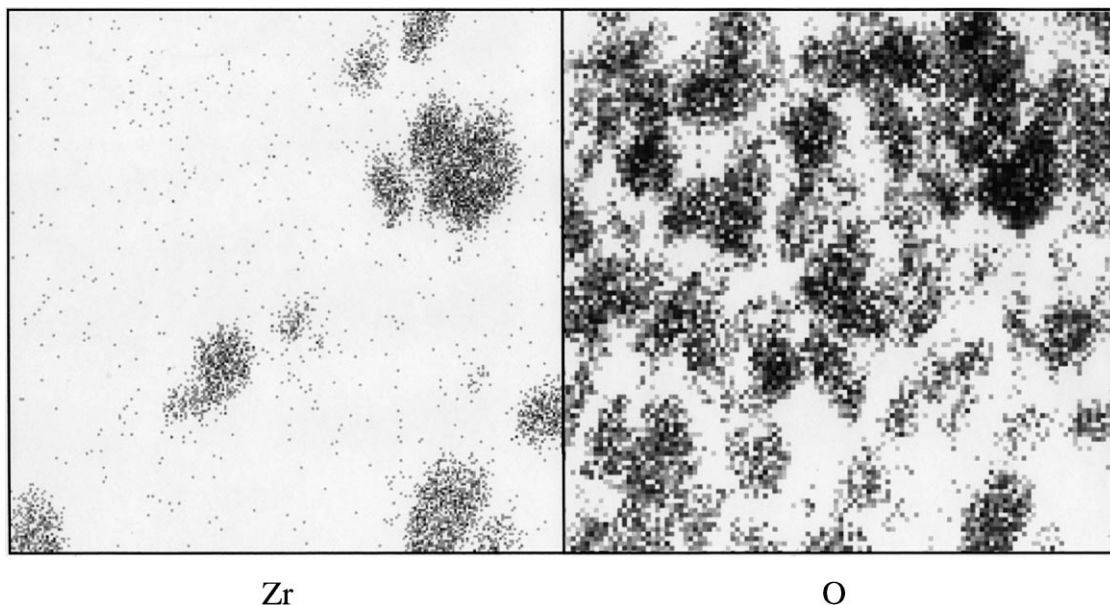


Fig. 5. Elemental maps of zirconium and oxygen obtained from the backscattering spectrum of Fig. 4. The total scan area is  $1 \times 1 \text{ mm}^2$ .

for oxygen makes it possible to measure oxygen in the presence of heavier elements. Regions around the surface energies for O and Zr were taken and are shown as a function of the beam position in the elemental maps of Fig. 5. The Zr maps agree very well with the maps obtained from the X-ray spectrum. However, they have much better statistics compared to the X-ray maps because of the high scattering cross section of the heavy elements.

The oxygen map of the measured region is not as clear as all the other maps. This is due to the background subtraction required to account for the energy overlap of particles scattered from the heavy elements. However, they still show the outline of most of the grains. In particular, the higher oxygen content in the zircon grains is clearly visible. Furthermore the complete absence of oxygen in pyrite grains is also apparent.

These results show that both X-ray fluorescence and high energy resonance can be used simultaneously to map both light and heavy elements. More important however is the fact that once elemental maps have been obtained, these can be used to perform spot measurements of selected regions. With these spot measurements quantita-

tive results for the oxygen content can be obtained from the well known calibration of the  $^{16}\text{O}(\alpha, \alpha)^{16}\text{O}$  resonance at 7.62 MeV [2]. This broad resonance can also be used to measure oxygen depth profiles.

### Acknowledgements

The authors would also like to thank Hans Noorman, David Garton and Alex Croal for their help in constructing the beamline and the Tandem Accelerator Operations Team for their efforts. We also wish to thank C. Waring for supplying us with the mineral sand sample.

### References

- [1] R. Siegele, D.D. Cohen, N. Dytlewski, Nucl. Instr. and Meth. B 158 (1999) 31.
- [2] J.A. Davies, F.J.D. Almeida, H.K. Haugen, R. Siegele, J.S. Forster, T.E. Jackman, Nucl. Instr. and Meth. B 85 (1994) 28.
- [3] F.J.D. Almeida, J.A. Davies, T.E. Jackman, Nucl. Instr. and Meth. B 82 (1993) 393.